

Supplementary materials to « Direct quantification of O-atom in low-pressure methane flames by using two-photon LIF” by Lamoureux, N. and Desgroux, P.

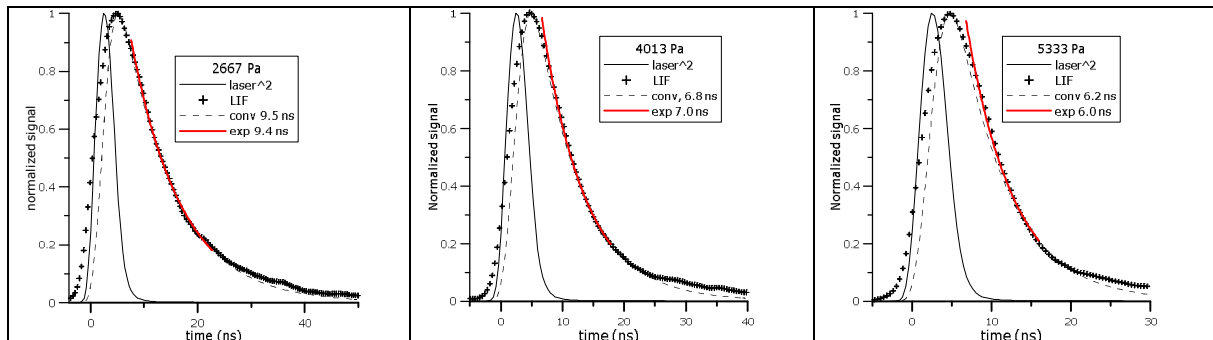


Fig. S0. Normalized temporal LIF signals of O measured (symbols) in stoichiometric $\text{CH}_4/\text{O}_2/\text{N}_2$ flame (flame $\text{CH}_4(100)$) at various pressure in Pa (see caption title). Also shown the squared laser pulse (thin black line) measured with the DET10A photodiode, its convolution with an exponential fit (dashed line), and the exponential fit between 90% and 20% of LIF intensity (red line). Fluorescence decaytimes obtained from the two fitting approaches are reported in each caption.

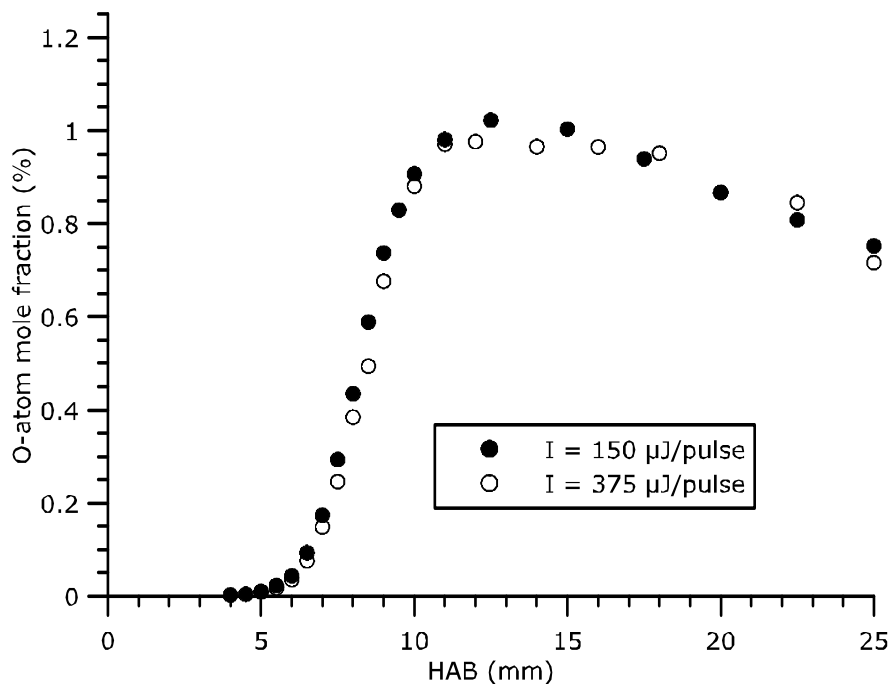


Fig. S1. Experimental O-atom profiles measured in flame $\text{CH}_4(080)$ with different laser intensities.

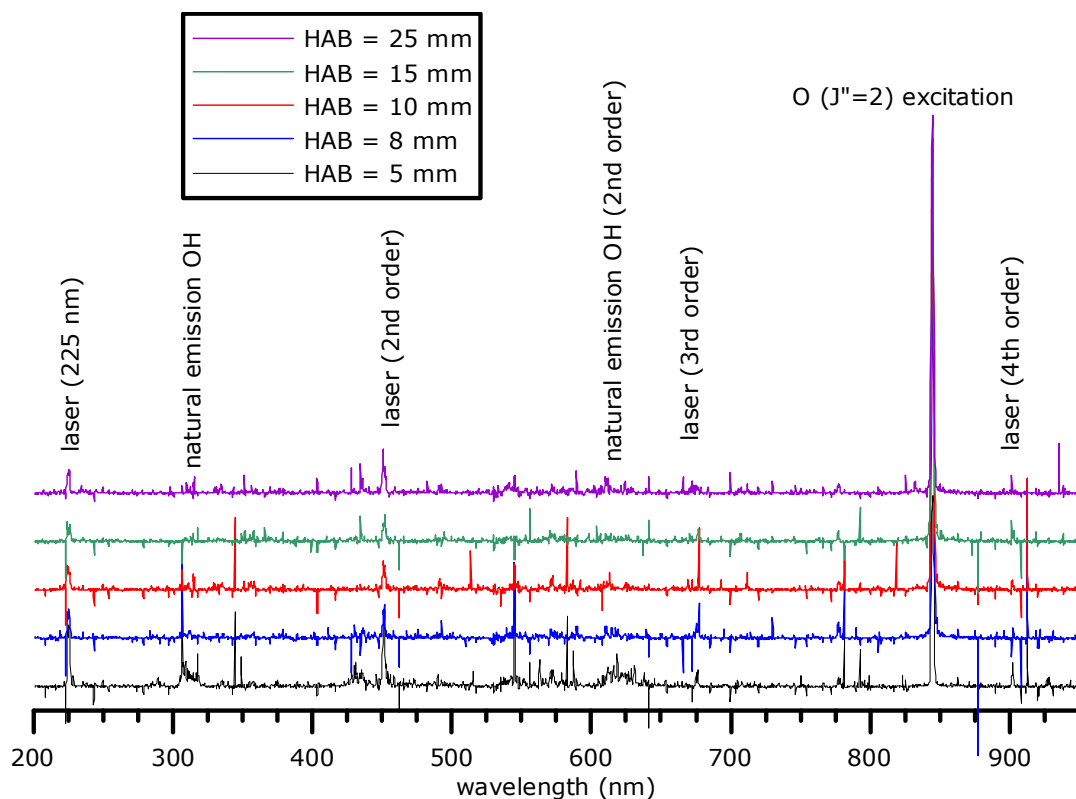


Fig. S2. Raw dispersed fluorescence spectra (not corrected for the natural emissions) measured at different HAB with the ICCD camera (gate = 150 ns) associated to a spectrometer using a 150 gr/mm grating blazed at 500 nm in flame CH₄(100).

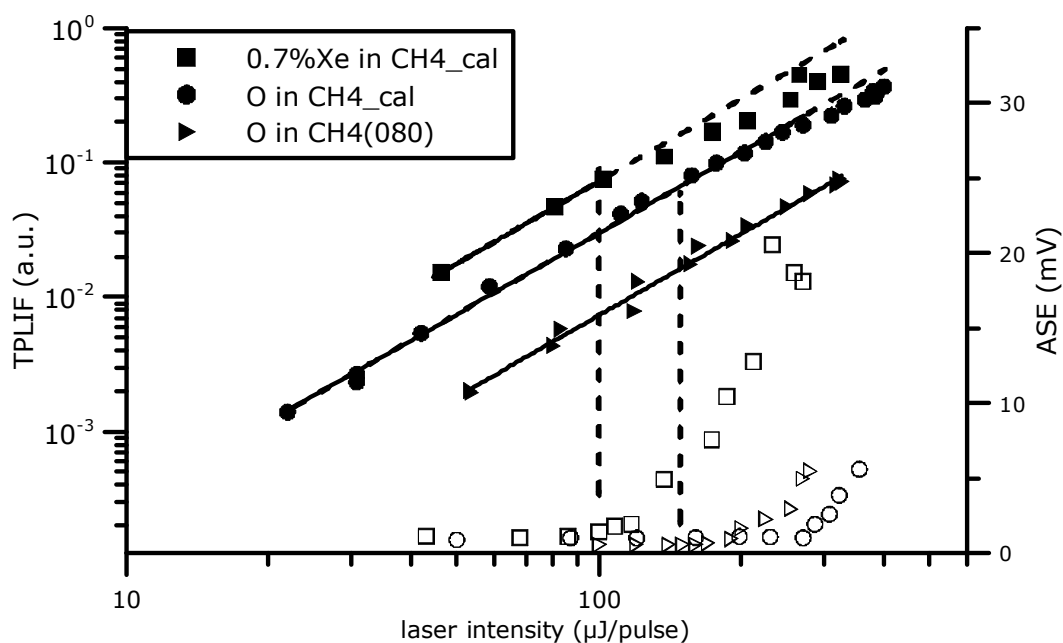


Fig. S3. TPLIF (closed symbols, in ln-scale) and ASE (open symbols, in normal scale) as function of the laser intensity for O and Xe in flames CH_{4_cal} and CH₄(080) at HAB=25 mm. Adapted from Fig. 3 presented in the main manuscript.

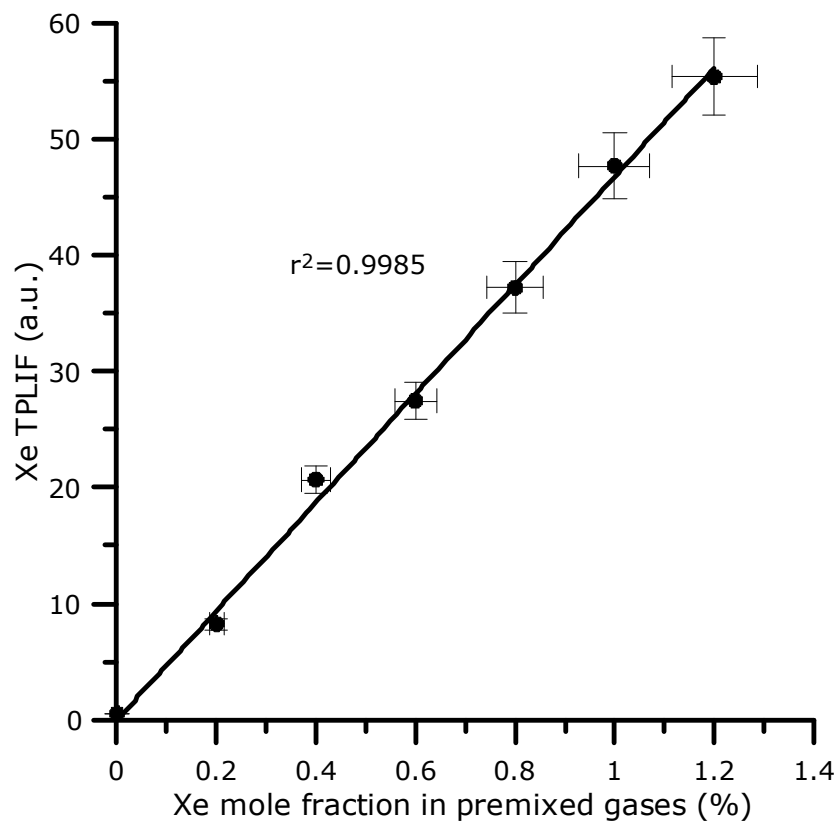


Fig. S4. Xe TPLIF signal in flame CH₄_cal (HAB=25 mm) as function of the mole fraction of Xe substituting Ar. Laser intensity = 90μJ/pulse.

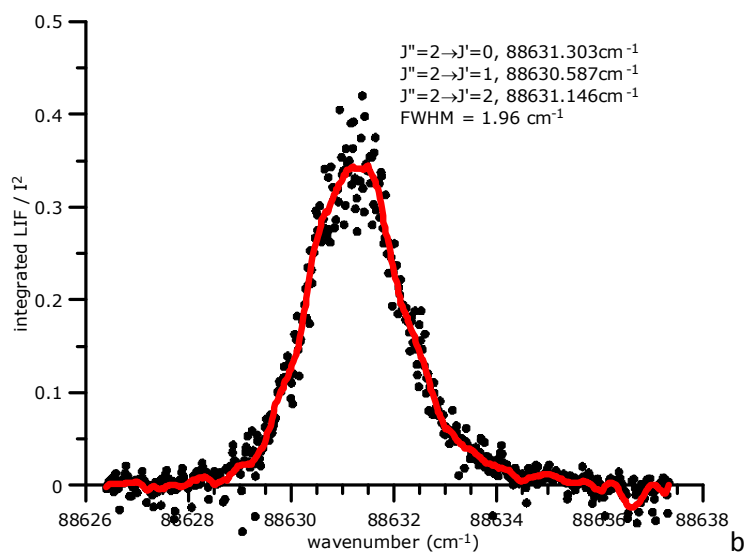
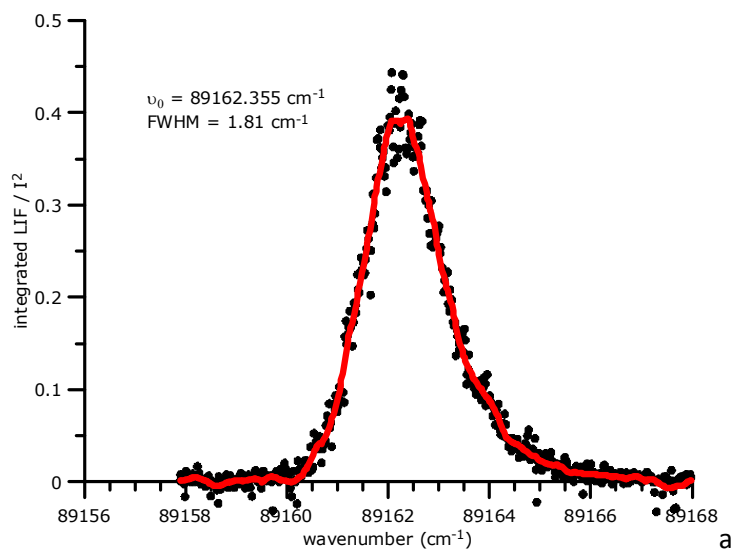


Fig. S5. Time integrated TPLIF line profiles measured at 30 mm in flame CH₄_cal (with 0.8%Xe) of a/ Xe, and b/ O-atom.

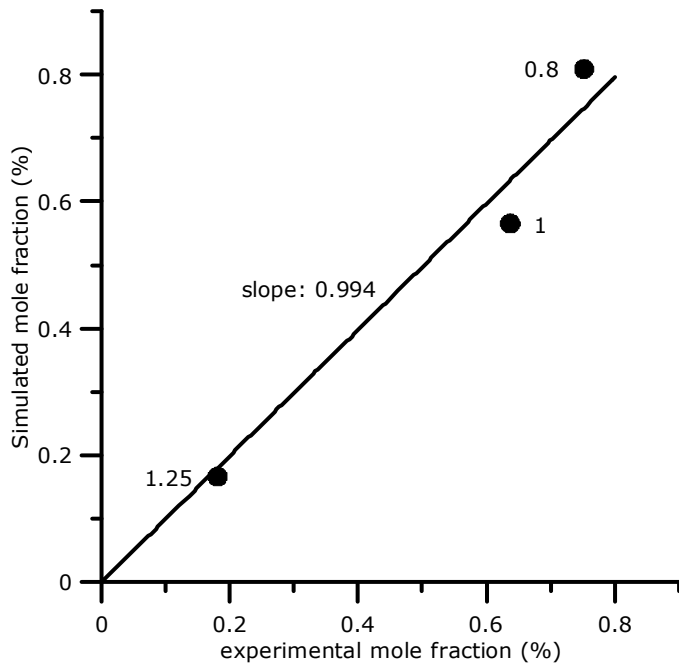


Fig. S6. Comparison between the experimental and the simulated O-atoms mole fractions at 25 mm in flames CH₄(080), CH₄(100) and CH₄(125). Labels beside symbols represent the equivalence ratio.

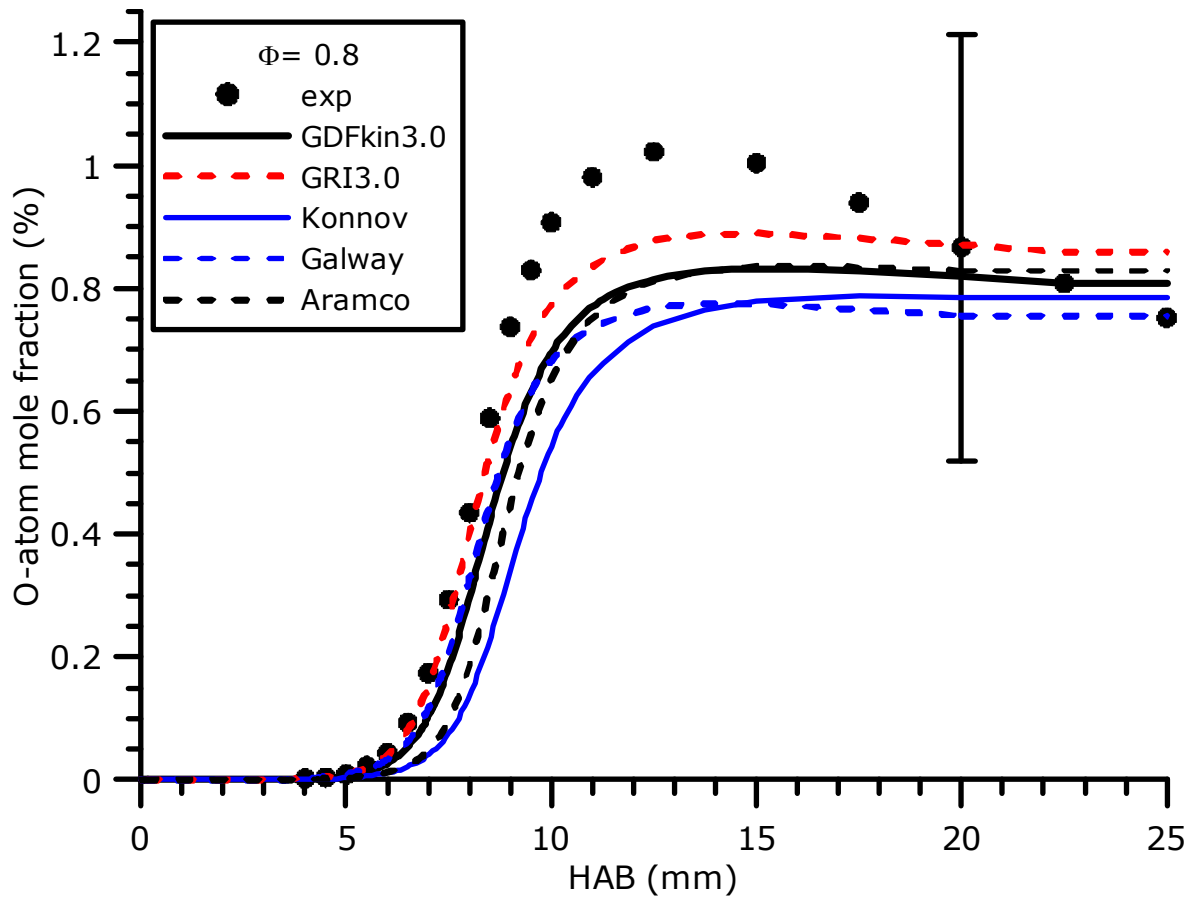


Fig. S7. Comparison between experimental O-atoms profile measured in flame CH₄(080) and the simulated ones by using Konnov [1], GRI3.0 [2], GDFkin3.0 [3], Aramco [4] and Galway [5].

- [1] A.A. Konnov, Implementation of the NCN pathway of prompt-NO formation in the detailed reaction mechanism, *Combust. Flame*. 156 (2009) 2093–2105.
- [2] G.P. Smith, D.M. Golden, M. Frenklach, N.W. Moriarty, B. Eiteneer, M. Goldenberg, C.T. Bowman, R.K. Hanson, S. Song, W.C. Gardiner Jr., V. Lissianski, Z. Qin, GRI-Mech3.0, GRI-Mech. (n.d.). <http://combustion.berkeley.edu/gri-mech/version30/text30.html>.
- [3] N. Lamoureux, H. El Merhubi, L. Pillier, S. de Persis, P. Desgroux, Modeling of NO formation in low pressure premixed flames, *Combust. Flame*. 163 (2016) 557–575. <http://dx.doi.org/10.1016/j.combustflame.2015.11.007>.
- [4] W.K. Metcalfe, S.M. Burke, S.S. Ahmed, H.J. Curran, A Hierarchical and Comparative Kinetic Modeling Study of C1 – C2 Hydrocarbon and Oxygenated Fuels, *International Journal of Chemical Kinetics*. 45 (2013) 638–675. <https://doi.org/10.1002/kin.20802>.
- [5] G. Bourque, D. Healy, H.J. Curran, C. Zinner, D.M. Kalitan, J. de Vries, C. Aul, E.L. Petersen, Ignition and Flame Speed Kinetics of Two Natural Gas Blends With High Levels of Heavier Hydrocarbons, *Journal of Engineering for Gas Turbines and Power*. 132 (2010) 021504.